Features of hydraulic fracture behavior for natural gas hydrate deduced from acoustic emission and microscopy in tri-axial fracturing experiments

Xian Shi[1,2,*], Weidong Zhang[1,2], Hongjian Ni[1,2], Caiyun Xiao[1], Haitao Zhu[1], and Shu Jiang[3,4]

[1] College of Petroleum Engineering, China University of Petroleum (East China), Qingdao 266580, PR China;

[2]Key Laboratory of Unconventional Oil & Gas Development (China University of Petroleum (East China)), Ministry of Education, Qingdao 266580, PR China;
[3]Key Laboratory of Tectonics and Petroleum Resources (China University of Geosciences (Wuhan)), Ministry of Education, Wuhan 430074, PR China;

[4]Energy & Geoscience Institute, University of Utah, Salt Lake City, UT 84102, USA;

Corresponding author: Xian Shi (xianshi@upc.edu.cn)

Key Points:

• In-situ stress and natural gas saturation affects fracture process and sediment mechanical properties
• Mixed fracture mode tends to be induced while micro fractures and craters were created due to phase change of gas hydrate
• Hydraulic fracturing most likely makes pathways favorable for natural gas hydrate

Abstract: The utilization of natural gas hydrate (NGH) as fuel is beneficial for meeting increasing energy demands. Hydraulic fracturing is a promising technology for developing NGH resources. Tri-axial fracturing experiments are combined with acoustic emission monitoring to study the feasibility of slickwater fracturing on NGH samples. The results reveal that the NGH samples with high gas hydrate saturation show better fracability; The fluid invasion zone can be found for samples with low gas hydrate saturation, indicating that micro fractures are created inside the sediment. In addition, the fracture morphology is more complex under the strike-slip fault regime than under the normal fault regime for all NGH samples, while a lower horizontal stress difference can increase the fracture complexity and breakdown pressure. The AE monitoring results shows mixed fracture modes exist during NGH fracturing, while the ratio of the tensile and shear fracture mode decrease with a large stress difference. Moreover, the post injection propagation can be observed due to the temperature related mechanical properties of the NGH sample; thus, the phase change of the solid gas hydrate is another important fracture mechanism for NGH fracturing, although the extent of the phase change's influence on the fracture behavior is closely related to the hydrate distribution and saturation. The fracture mechanical stability observation shows a more rapid strength decrease and large deformation and failure for the NGH samples with high gas hydrate saturations, although the effectiveness is high; thus, it is necessary to balance natural gas production with the geological risk before fracturing.

1. Introduction

With the rapid development of industry and the economy, the demands for energy resources are

increasing worldwide. The natural gas deposited in natural gas hydrates (NGH) can serve as an appropriate substitute for conventional fossil fuels, such as oil and goa, as it is a comparatively abundant energy source. Recent estimates indicate the amount of carbon stored in NGH resources is equivalent to twice the amount of carbon found in all other fossil fuels (Chong et al.,2016; Piñero et al.,2013). Natural gas hydrates are crystalline solids with methane molecules enclosed under special thermodynamic conditions. Currently, NGH resources are mostly found in harsh environments, such as deep oceans and permafrost regions. Because of the special phase equilibrium properties of gas hydrates, the gas extraction from the NGH resource generally needs to break the thermodynamic conditions by shifting the pressure and temperature. However, field trails on NGH development show that the gas production rate cannot meet the commercial demand. Thus, developing effective and safe production strategies for natural gas recovery from NGH reservoirs are great challenges in the oil and gas industry.

The methods for developing NGH have received much attentions in recent years. In general, the current development methods for NGH can be classified into several categories. The most commonly used is the depressurization method, which requires the NGH occurrence system pressure to decrease to dissociate pressure. Because of the simple implementation and relatively low cost for engineering operations, the depressurization method is the only method that has been conducted in several small scale commercial projects (Oyama et al.,2009; Xu & Li,2018). However, because the lack of continuous support and because this method independently relies on natural NGH dissociation, the gas production rate from the depressurization method is not ideal (Chen et al.,2019; Li et al.,2014). Alternatively, thermal stimulation is another method proposed for NGH, as heat injection can also stimulate the thermodynamic balance conditions at a faster rate. In general, well heating and hot water injection heating production are two commonly used approaches in thermal stimulation methods. However, because the thermal stimulation methods are sometimes only effective for the dissociation reaction near the wellbore, it is still not an economically feasible approach (Falser et al.,2012; Zhang et al.,2019). Inhibitor injection is another type of NGH stimulation method that works by preventing gas hydrate formation or aggregation. Chemicals, such as methanol, mono ethylene glycol, and salts, can be injected to boost the NGH dissociation, but the highly corrosive and volatile characteristics of the chemicals are great threats to the environment if the residual toxic chemicals cannot be retrieved (Cranganu,2009; Qazi et al.,2020). CO_2 replacement is an attractive production method because the exchange CO_2 with external CH_4 does not require hydrate dissociation. Furthermore, the injection CO_2 into NGH resources can be considered an attractive solution for greenhouse gas capture. However, the low rate of hydrate generation and the low gas consumption restrict commercial applications of the CO_2 replacement technology (Atousa & Kiana,2020; Yohan et al.,2017). In recent years, some authors have suggested that combining these methods is potentially cost effective and efficient method for actual NGH exploitation, although the economic viability of this method has only been tested in labs in most cases (Song et al.,2015; Fakher et al.,2018). Because of the advantages and disadvantages of the current NGH stimulation methods, how to commercially develop NGH effectively and safely is still a debatable topic. According to the latest data, the field methane hydrate production tests that have been performed have been of limited duration, i.e., from 6 to 25 days (People's Daily,2017; Boswell & Collett,2011). Thus, how to keep the gas production rate at a sufficiently high level is the key for sufficient gas production for NGH development.

Hydraulic fracturing is a stimulation technology that artificially creates fractures to improve

permeability by injecting viscous fluids into the target formation, and it has played an important role in the rapid increase of oil and gas production from unconventional hydrocarbon resources (Zhang et al.,2017; Rachel et al.,2017). Compared to the small scale contact area near the wellbore, the created hydraulic fracture or fracture network system can extend far from the wellbore. Thus, the temperature and pressure in large zones of NGH resources can be the disrupted and stimulated, which can facilitate the rapid decomposition of the gas hydrate. In addition, the high flow conductivity hydraulic fracture will also improve the fluid migration, speed up the heat and mass transfer efficiency and the pressure drop rate, thus effectively stimulating the natural gas production. The conceptual model of the fracturing mode of the hydrate reservoir is shown in Fig. 1. To validate the feasibility of hydraulic fracturing in NGH development, some pioneer work has been carried out by various authors. Jin et al., 2015 analyzed the vertical fracture propagation due to the natural gas hydrate decomposition; they found that the hydrate decomposition rate, Young's modulus and fracture toughness of the hydrate sediments were the main influencing factors that control the fracture propagation (Jin et al., 2015). Konno et al., 2016 applied low temperature hydraulic fracturing equipment and X-ray computed tomography to observe the fracture initiation, propagation and permeability change before and after stimulation. They demonstrated that hydraulic fractures can be a conducive channel to improve the hydrate decomposition rate and ensure the final gas production. In particular, sufficient permeability can be guaranteed even after the fracture closure, which will potentially extend the production time (Konno et al., 2016). Chen et al., 2017 applied the TOUGH+HYDRATE simulator to examine the production efficiency of hydraulic fracturing in NGH development. They found that the natural gas production rate and cumulative production are greatly improved with fracturing. Furthermore, by adjusting the fracture quantity and spacing, there is an optimum fracturing scenario (Chen et al., 2017). Wang et al., 2018 established a temperature model for gas hydrate dissociation after fracturing stimulation in NGH formation. They indicated that the fracture geometry can affect the temperature distribution of the hydraulically fractured zone, while there are different zones apart from the fracture distance; thus, optimization of the fracturing fluid is necessary (Wang et al.,2018). Too et al., 2018a measured the apparent fracture toughness of frozen sand using hydraulic fracturing in a penny-shaped crack. Three methods for fracture toughness, namely, the stress-intensity factor (SIF), Volume-SIF and brittleness approach, were compared (Too et al., 2018a). Too et al., 2018b conducted hydraulic fracturing experiments under high pressure and low temperature conditions, and the experimental results show the feasibility of creating artificial fractures in synthetic methane hydrate-bearing sand (Too et al.,2018b). Feng et a., 2019 used a numerical approach to demonstrate the effectiveness of the combination of hydraulic fracturing and the depressurization method in NGH; they also discussed the temperature of the target NGH reservoir on the gas production rate and finally indicated the high efficiency of this integrated method (Feng et al.,2019). According to previous studies, there are still many problems with unclear solutions, especially the fracture mechanisms for fracture initiation and propagation under different stress regimes. Moreover, the effect of the gas hydrate saturation on the fracture behavior of methane hydrate-bearing sand is relatively rare, although the mechanical properties of the NGH sediment sample depend closely on the gas hydrate saturation.

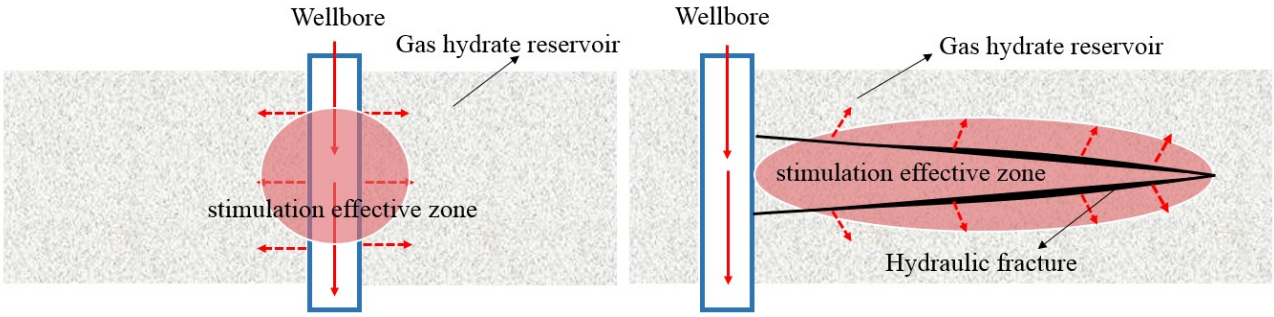

Fig.1 The comparison of conventional stimulation and fracturing stimulation for gas hydrate reservoir

Thus, a series of experiments were performed with a true triaxial hydraulic fracturing instrument and an acoustic emission monitoring system under high pressure and low temperature conditions. The synthetic gas hydrate samples were prepared according to the physical parameters of gas hydrate from the South China Sea, while saline water is used as the seawater-based fracturing fluid. In addition, the effects of the gas hydrate saturation, horizontal stress difference and in situ stress regimes on the initiation pressure and propagation were investigated. Finally, microscopic image observation was used to observe the creation of the hydraulically fractured closure with time after hydraulic fracturing. This work provides a closer examination of the fracture initiation and propagation process for the NGH samples. Furthermore, the experimental results for this process are valuable to furthering the completion of a design and stimulation strategy for field NGH stimulations using hydraulic fracturing.

2. Experiments

2.1 Apparatus

In this research, all the experimental equipment (except computer and control cabinet) are placed in a self-developed low-temperature controlled laboratory (Emerson microcomputer freezing control system, refrigeration temperature: 50°C ~ 20°C), as shown in Fig. 2(a) and Fig. 2(b). The movable true triaxial hydraulic fracturing experimental device is placed in the laboratory and it is mainly composed of a true triaxial servo system, a stress loading system, a constant speed constant pressure pump Teledyne S65DM, a data acquisition system, a pipe valve, and auxiliary devices, etc. The tri-axial test frame is able to exert independent stresses of up to 50 MPa on the test block in three principle directions. The acoustic emission detection system is the AMSY-5 acoustic emission system that includes sensors, preamplifiers, and data acquisition cards, which are all manufactured by Vallen Ltd. A total of 8 acoustic emission probes are equipped in this hydraulic fracturing experiment. The threshold value of the AE amplitude analysis system was 40 dB and the sampling frequency was 10 MHz. During the experiment's processes, the data for the axial stress, confining pressure, fluid pressure, temperature, acoustic emission, and strain were monitored and recorded by real-time data acquisition software in a DELL T7810 workstation.

2.2 Sample preparation

According to the previous investigation, it was found that the sediment skeleton in the South China Sea area was argillaceous siltstone with a silty content of 72%-82%. The particle size of silty sand was mainly 8 ~ 63 m, and the median particle size of the formation was approximately 50 m. Therefore, in the preparation of the hydrate fracturing samples, the unconsolidated skeleton particles are selected as quartz sand with the mesh numbers selected ranging from 30 to 200 mesh

and 70 to 400 mesh.

In the process of hydrate formation, the temperature of the hydrate reactor is reduced by setting the pressure environment and utilizing the circulating refrigeration system. The pure CH_4 gas (99.9%) used in this study was supplied by Qingdao Tianyuan Gas supply Ltd. Generally, the metering room is filled with CH_4 gas in the range of 8 to 10 MPa, and parameters such as the inlet pressure, resistivity, time difference and wave velocity of the reaction kettle can be recorded. The steps of the gas injection are repeated so that all the deionized water in the reaction kettle can form gas hydrate. Deionized water was used to form the NGH and to create an aqueous-rich environment during the NGH formation. When the hydrate pattern is prepared with different saturations, the degree of hydrate saturation can be determined by controlling the amount of water. To assure the stability of the artificial gas hydrate, the hydraulic fracturing samples generally need a preparation time of at least 10 days.

Finally, a total of 8 hydrate fracturing NGH samples of 100 mm×100 mm×100 mm with different saturations were formed, which were marked as No. 1 to No. 8 (see Fig.2(c)). High-strength steel tubes with outer diameters of 14 mm and inner diameters of 10 mm were placed in the middle of sample to simulate perforations. The No.1 to No. 4 samples exhibited experimental fracturing patterns of highly saturated gas hydrate sediments, and the gas hydrate saturation percentages were approximately 80%. The No. 5 ~ 8 samples exhibited relatively low saturated gas hydrate sediment fracturing experiment patterns, and the gas hydrate saturation percentages were approximately 40%.

(a) **(b)**

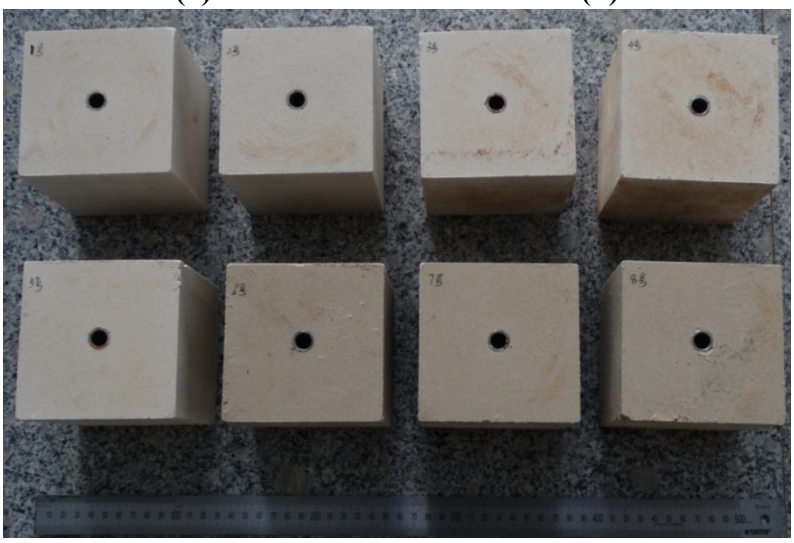

(c)

Fig. 2 Schematic of the true-axial experimental system for NGH samples

2.3 Experimental design

To simulate the hydraulic fracturing of NGH reservoirs in a vertical well, the direction of the wellbore is consistent with the overburden stress (σ_v), and the maximum horizontal principal stress (σ_H) and minimum horizontal principal stress (σ_h) are applied on both sides of the sample. Because the ocean NGH reservoirs existing in shallow formations are good candidates for development with the current existing techniques, the geological in situ stress values were set with a close difference between the overburden pressure and two horizontal principle stress values in this study. Two in situ geological stress regimes, namely, the normal fault regime ($\sigma_v > \sigma_H > \sigma_{h)}$ and strike-slip fault regime ($\sigma_H > \sigma_v > \sigma_h$), were set during the hydraulic fracturing testing. To improve the observation of the fracture morphology after fracturing, a blue tracer was added to the fracturing fluid, in which the fracturing fluid was saline water with viscosity of 5 mPa·s and the salt concentration was 3.5% in weight. In the experiment, the overburden stress was first applied, and then the maximum and minimum principal horizontal stresses were applied. After the stress condition was applied, the fracturing fluid was injected until the fracturing sample was finally broken. The injection rate of the fracturing fluid was set at 100 ml/min. After the completion of the hydraulic fracturing experiment, the sample was cut and the fracture morphology observed; additionally, the pumping pressure and acoustic emission data were processed and analyzed. The detailed experimental design scheme is shown in table 1.

Table.1 True axial hydraulic fracturing experimental design for the gas hydrate bearing sediment samples

Sample number	In situ stress type (MPa)	Horizontal stress Difference (MPa)	Gas hydrate saturation (%)	In situ stress type
No. 1	σ_v =7-σ_H =6-σ_h =4	2	80%	Normal stress regime
No. 2	σ_v =7-σ_H =6-σ_h =6	0	80%	Normal stress regime
No. 3	σ_v =6-σ_H =7-σ_h =5	2	80%	Strike-slip stress regime
No. 4	σ_v =6-σ_H =7-σ_h =6	1	80%	Strike-slip stress regime
No. 5	σ_v =7-σ_H =6-σ_h =4	2	40%	Normal stress regime
No. 6	σ_v =7-σ_H =6-σ_h =6	0	40%	Normal stress regime
No. 7	σ_v =6-σ_H =7-σ_h =5	2	40%	Strike-slip stress regime
No. 8	σ_v =6-σ_H =7-σ_h =6	1	40%	Strike-slip stress regime

3. Experimental results and analysis

3.1 Fracture morphology of the hydraulically fractured NGH samples

Fig. 3 shows the fracture morphology of hydrate sediments after the true triaxial fracturing experiment. Considering that the created hydraulic fracture would lead to a rapid decomposition of the gas hydrate, all the fracture morphology images were collected immediately after the completion of the hydraulic fracturing tests. Fig. 3(a) shows the fracture morphology under two different saturation conditions after fracturing when the sample was excavated to half; it can be seen that an obvious hydraulic fracture can be found on the top surface of the No. 2 sample with the high gas hydrate saturation content. For comparison, no fracture appears on the top surface of the No. 8 sample with the low gas hydrate saturation. In addition, a clear fluid invasion zone with a blue tracer distribution can be observed, which indicates the large fluid loss of the low viscos fracturing fluid for the sample with low gas hydrate saturation. Because of the dissipated energy near the wellbore, it is difficult for the hydraulic fracture to propagate toward the boundary. One possible reason is that the viscosity of the slickwater fracturing fluid is low. Thus, the fracture morphology of the sample with the low gas hydrate saturation seems to be similar to that of unconsolidated sand. Fig. 3(b) shows the fracture morphology of all the NGH samples after the samples were excavated to half.

When comparing the fracture morphologies of all the hydrate fracturing samples under different saturations, a main vertical hydraulic fracture can be found after cutting them. However, there are some differences for the secondary fractures. More obvious secondary fractures and micro fractures can be found for the sample with the high gas hydrate saturation, whereas it is difficult to directly observe the secondary fractures for the NGH samples with low gas hydrate saturation with the naked eye. The close observations of the blue tracing agent on the sample surfaces also indicated that the blue tracer fracturing fluid was mostly found in the surrounding area of the wellbore and the seepage zone was limited for the NGH samples with high gas hydrate saturation, which reflected that the energy release was concentrated and the fractures generated during the sample fracture were more likely to reach the boundary. In contrast, the blue tracer fracturing fluid is more evenly distributed on the fracture surface for NGH samples with low gas hydrate saturation, thus forming a larger fluid invasion area. The wide distribution of fracturing fluid reflects the relatively dispersed energy release and larger leak-off rate; thus, the hydraulic fractures have difficulty directly propagating towards the boundary for the NGH samples with low gas hydrate saturation. In general, the brittleness of the NGH sample is positively related to the gas hydrate saturation, which is because increasing the gas hydrate can improve the NGH sediment strength.

The in situ stress regime and horizontal stress difference play significant roles in the hydraulic fracture initiation and propagation. When comparing the hydraulic fracturing results for the NGH samples under different conditions, it can be seen that the fracture geometry for the samples (No.1, No.2, No.5 and No.6) under the normal fault in situ stress regime is a relatively simple vertical fracture, but the fracture geometry for the samples (No.3, No.4, No.7 and No.8) under the strike-slip fault regime is the combination of vertical and nonplanar fractures. The occurrence of a more complicated fracture morphology for the sample under the strike-slip fault regime results from the close difference between the overburden stress and the two horizontal stress, especially when the overburden stress is the intermediate principal stress state; thus, torturous fractures can be created

due to the complex stress redistribution near the wellbore. In addition, the fracture propagation deviation degree is more evident for the samples with high gas hydrate saturation, such as samples No. 2 and No. 4. The further observation of sample No. 4 indicated that hydraulic fractures not only propagated along the minimum horizontal stress direction but also reoriented to the minimum horizontal stress direction. In general, the fracture morphology of the NGH sample tends to be simpler while the fracture size is also larger and can be easily observed. In addition, the fracture morphology becomes more complex with the increase of the gas hydrate saturation. The fracture morphology is more complicated under the strike-slip fault regime condition, while a lower stress difference could further increase the complexity of the fracture system. In contrast, the fracture morphology under the normal fault condition and high stress difference mainly produces simple planar fractures after the fracturing stimulation.

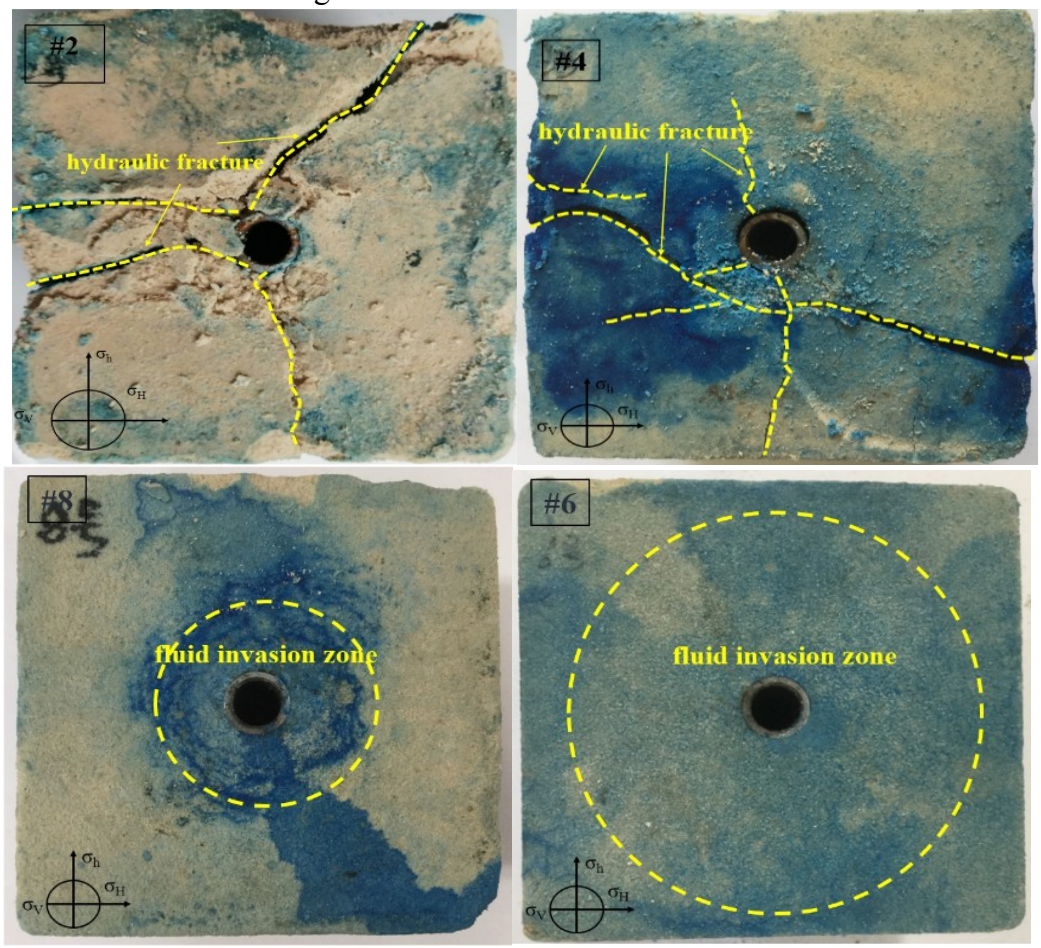

（a）Top view for NGH fractured samples

（from left to right：No.2，No.4，No.6 and No.8）

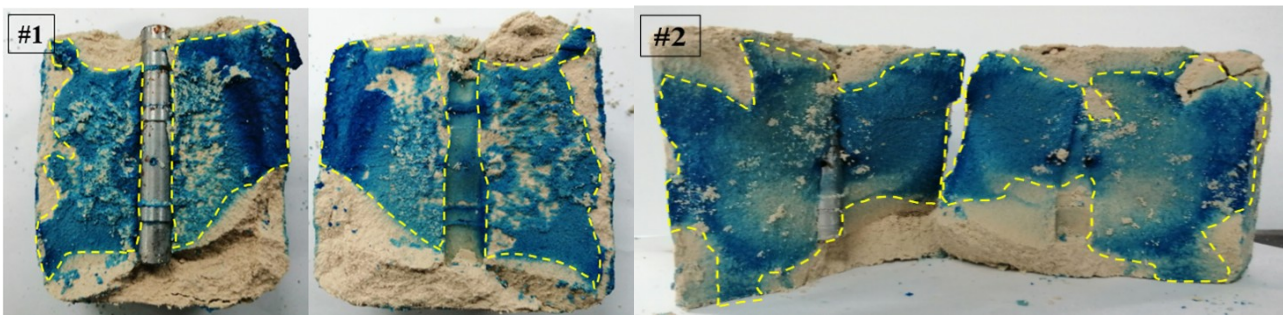

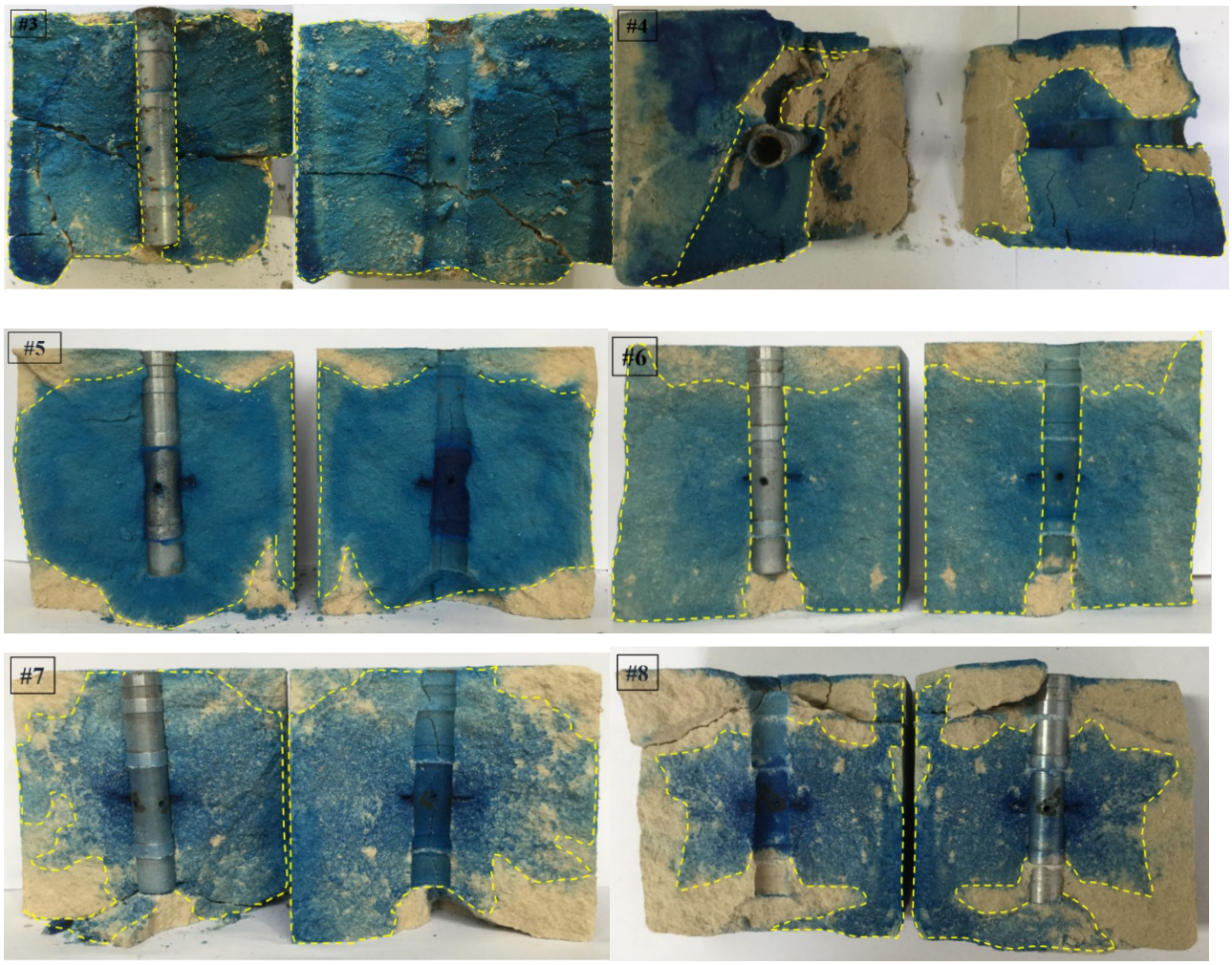

(b) Fracture morphology after cutting

Fig. 3 Hydraulic fracture geometries of the NGH samples after the hydraulic fracturing experiments

3.2 Injection pressure and AE energy rate versus time curves

The curves of the pump pressure and acoustic emission (AE) energy changing with time during the true triaxial fracturing of the NGH sediments with high gas hydrate saturation under the normal fault regime are shown in Fig. 4. Fig. 4(a) shows the pump injection pressure and AE energy curve with time for sample No. 1; it can be seen that the change of the pumping pressure curve is similar to that of brittle rock; there is a sharp pressure rise near the pressure peak, which refers to the breakdown pressure, which then rapidly declines until the fracture stops growing. When the sample is fractured near the breakdown pressure point, there is an obvious enhancement of AE energy. For this sample, the breakdown pressure is approximately 18.83 MPa. Fig. 4(b) illustrates the change curve of the pumping pressure and acoustic emission energy of sample No.2 with high hydrate saturation under the normal fault regime. The trend of the curve is similar to that of sample No. 1. The breakdown pressure of this sample is 20.92 MPa, which is higher than sample No. 1. Fig. 4(c) and 4(d) show the change of the injection pressure and AE energy curve for No. 3 and No. 4 with relatively low gas hydrate saturation under the strike-slip fault regime. It displays that the injection pressure curve trend of sample No. 1 is similar to that of sample No. 3, while the curve trend of sample No. 2 is similar to that of sample No. 4. However, there is great change in the breakdown pressure; the breakdown pressure of sample No. 3 was 32.11 MPa, while the fracture pressure was

32.11 MPa, which is larger than the other high gas hydrate saturated samples under the same conditions, except for the in situ stress regime.

Fig. 4(e) the shows injection pressure and AE energy curve of sample No. 5 with low hydrate saturation under the normal fault regime. According to the experimental results, the pumping pressure curve raised slowly at the initial stage and climb to the breakdown pressure, then the injection pressure drops rapidly when the injection stop. It is evident that there is an injection pressure platform after the injection pressure reached the breakdown pressure point, indicating that extending the hydraulic fracture is difficult. The breakdown pressure of this sample is 19.82 MPa; Fig. 4 (f) shows the curve change of the injection pressure and AE energy of sample No. 6 with low gas hydrate saturation under the normal fault regime. From the paragraph, the trend of this sample is similar to the curve of sample No. 5. The breakdown pressure is 26.98 MPa. Fig. 4(g) and 4(h) show the curve changes of the injection pressure and AE energy of the No. 7 and No. 8 samples under the strike-slip regime. It can be seen that the there are certain similarities regarding the pressure curve change; the breakdown pressures of samples No.7 and No.8 were 27.54 MPa and 28.70 MPa, respectively. Among all the samples with low gas hydrate saturation, the breakdown pressure of sample No. 8 is also the highest.

Basically, it can be found that the entire injection pressure and AE energy curve can be divided into three stages, namely, micro fracture creation, microscopic fracture initiation and fracture growth till stop. According to the characteristics of the AE energy signals, it can be seen that the intensity of the AE activities was relatively small at the beginning of the injection when the fracturing fluid was first pumped, and AE activities surge before and after the fracture breakdown. Interestingly, the AE activities also increase greatly after the breakdown even if the injection stops. Different from the other sedimentary rocks, the intense AE activities not only occur near the breakdown but also occur randomly during all fracturing processes. In particular, for some samples, the AE activities after the injection stops are more intense than in the other injection periods. In general, the surge of AE activities indicates fracture initiation behavior; thus, the fracture initiations for NGH samples could occur in many locations. In general, the fracturing fluid immersed fracture can be regarded as a "wet" fracture, while a fracture without fracturing fluid refers to a "dry" fracture. Thus, fracture initiations in these areas might belong to "dry" fractures without fracturing fluid but result from self-mechanical property changes due to rapid gas hydrated dissociation and local stress concentration release.

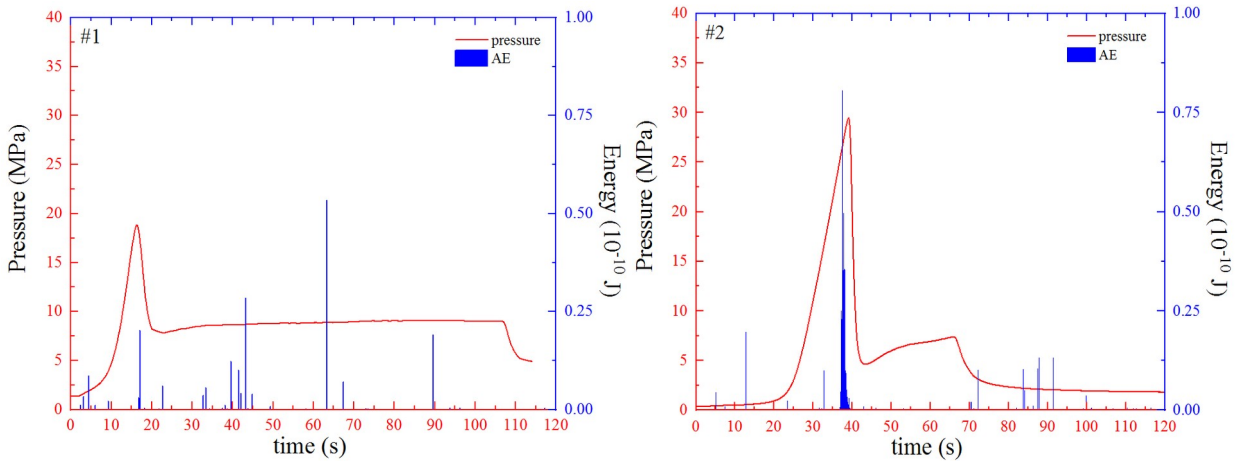

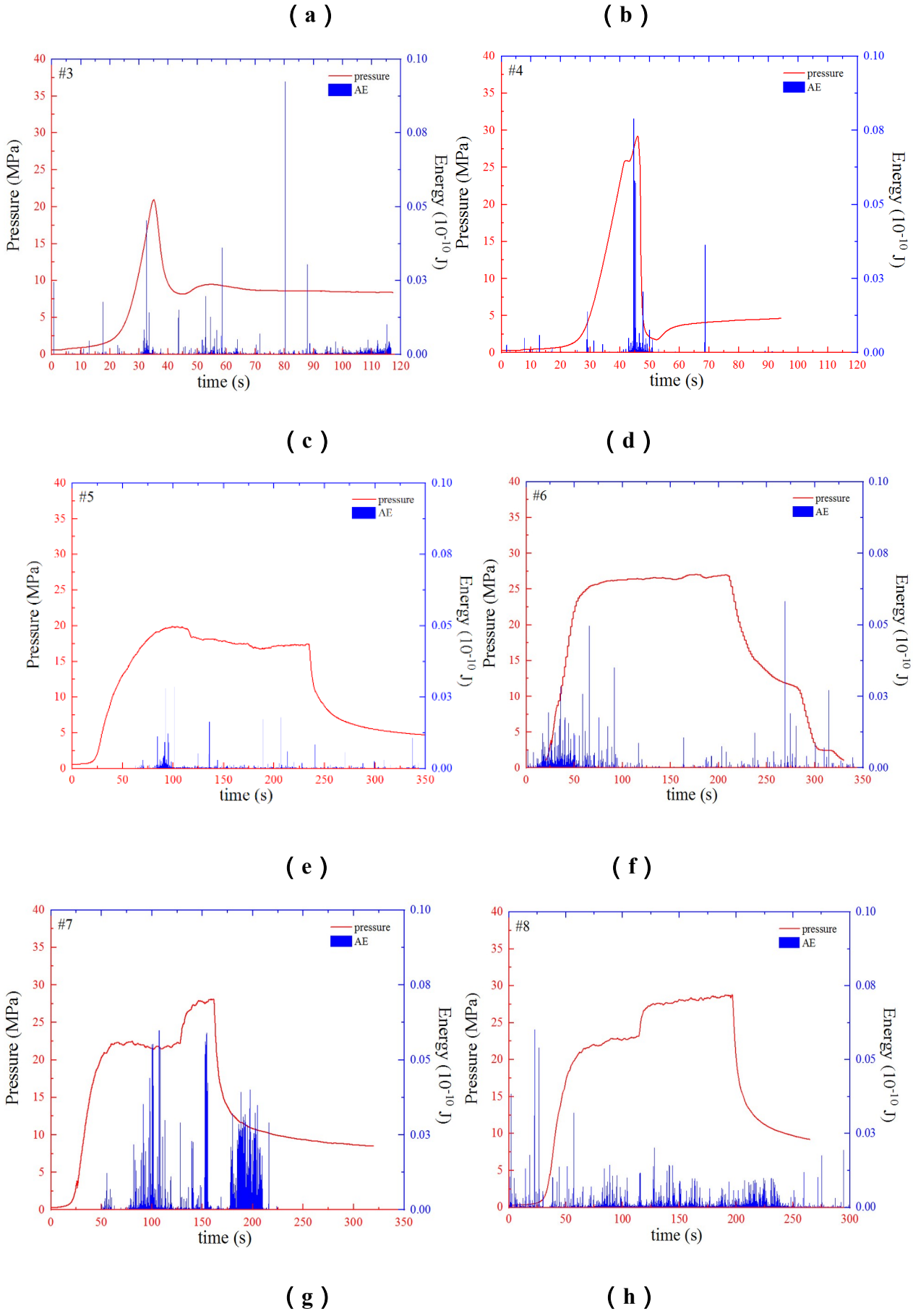

Fig. 4 Injection pressure change curve and acoustic monitoring results for the NGH samples

under the tri-axial fracturing condition

3.3 Time vs. space AE monitoring results

The application of AE is a powerful tool to study the mechanical properties of rock by examining the elastic wave emitted during loading. The AE data density not only represents the fracture extension area but also reflects the permeability and porosity at this location to a certain extent (Jin et al.,2015; Konno et al.,2016). Fig. 5(1) and 5(2) illustrate the space-time AE evolution characteristics of the NGH samples with different gas hydrate saturation percentages. According to the experimental results of the samples with high gas hydrate saturation values, the AE activities occur mainly in three directions and increase in an orderly manner along these directions. Additionally, more AE activities can be found at the bottom of this sample, indicating that the microscopic hydraulic fractures tend to occur initially at the bottom and then extend to the boundary. The three dimensional AE evolution also showed that the AE activities distribute discretely around the wellbore, indicating less intensive energy dispersion during the fracturing. Generally, the created hydraulic fractures were controlled mainly in the in situ stress direction. For the sample with low gas hydrate saturation, the AE activities distribute centrally near the wellbore but tend to distribute to larger areas than the sample with high gas hydrate saturation after the injection stops, which is probably due to the high leak-off rate. Moreover, the combination of AE activities and the fracture after cutting the sample shows that this type of AE activity belongs to a large number of micro fractures. In other words, energy dissipation is large near the wellbore for the sample with low gas hydrate saturation; thus, creating microscopic fractures is difficult, while the created hydraulic fracture direction tends to be uncontrolled by the in situ stress direction. From the space-time evolution results of the sample with high gas hydrate saturation, there is an obvious difference under the three specific time scales. The AE activities increase significantly over time. Conversely, the change for the space-time evolution for the sample with high gas hydrate saturation is not evident. Before the injection time of 30 s, many of the AE activities were already observed.

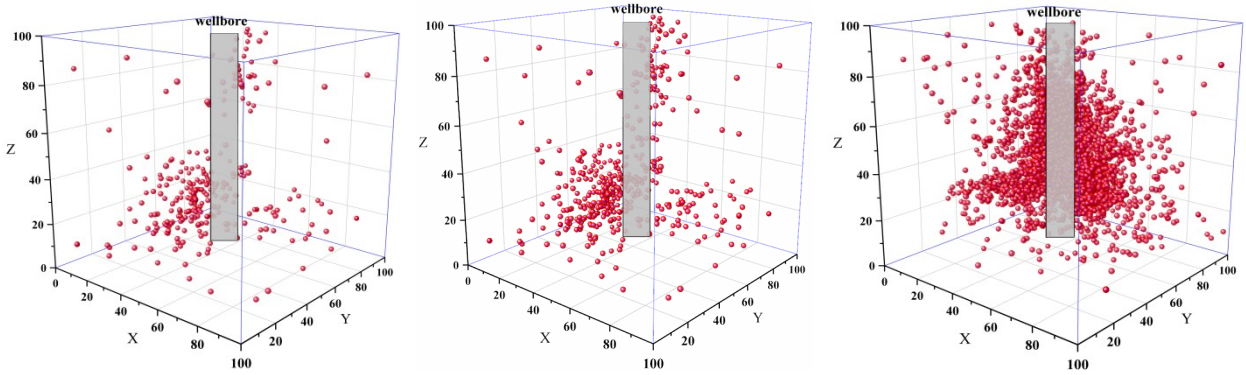

(20 s) **(40 s)** **(120 s)**

(a) NGH sample with high gas hydrate saturation (sample No. 2)

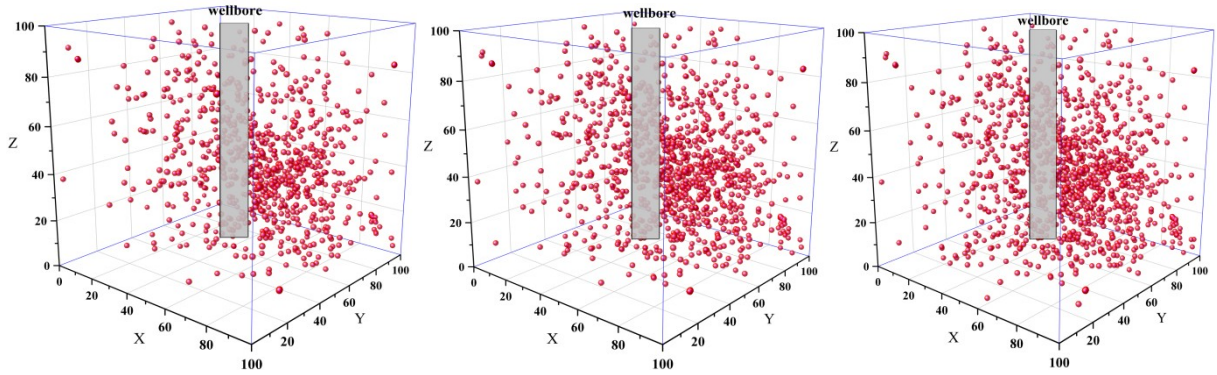

(30 s) (220 s) (350 s)

(b) NGH sample with low gas hydrate saturation (sample No. 6)

Fig. 5 Time vs. space AE monitoring results for gas hydrate bearing sediment during hydraulic fracturing

4. Discussion

4.1 Hydraulic fracturing mechanisms for NGH fracturing

Basically, according to the injection pressure and AE change curve, the entire injection process can be divided into the following four stages: prefracture initiation, fracture initiation, fracture extension with injection and fracture extension post injection. The comparison of the injection pressure curves for the NGH samples with high gas hydrate saturation and low gas hydrate saturation indicate that these curves are different. For the sample with high gas hydrate saturation, the injection pressure generally dropped rapidly after the breakdown pressure was reached, whereas there is a platform for the extension pressure for the sample with low gas hydrate saturation. Moreover, the pressure curve of the NGH sample with low gas hydrate saturation follows an increasing trend with more fluctuations than that of the NGH sample with high gas hydrate saturation, which indicates that large energy dissipation occurs during the initiation stage and that there are secondary fractures created during the fracture extension process. Except for that, the injection of the breakdown pressure also has a close relationship with the in situ stress condition. In particular, there is second increase in the injection pressure in most cases for the samples under the slip-strike regime, indicating fracture reorientation and secondary fracture creation, which matches with the fracture cut observation. For NGH samples with the same gas hydration saturation, the breakdown pressure is higher under the normal fault regime than under the slip-strike fault regime. Moreover, a lower principle stress difference could increase the breakdown pressure under the same in situ stress regime. The application of AE monitoring technology can be used to explain the fracture mechanism with time. The comparison of the AE energy and three location data reveal that the AE signals surge not only before and after breakdown pressure but also during the extension stage post injection. Moreover, the AE signals seems to be more widely distributed on both the spatial and temporal scales. Indeed, the less brittle mechanical properties and high leak off-rate of the NGH samples should account for this behavior. The comparison of the breakdown time shows that samples with low gas hydrate saturation tend to need more time for energy accumulation during the fracture initiation, which can also show the lower fracability response for samples with low gas hydrate saturation. In contrast, the breakdown times for samples with high gas hydrate saturation are less than 50 s, displaying a good fracability.

Unlike sedimentary rocks, the coupled effect of the gas hydrate decomposition, hydraulic fracture deformation and fluid flow affect the fracture initiation and extension process. Thus, the phase change of the gas hydrate is the possible mechanism for NGH fracturing. During the fracturing initiation and propagation process, NGH crystals may suffer from damage may be crushed due to the great increase of strain. Because the cementing effect of solid gas hydrate within NGH sediment is gradually destroyed under the strain, while the temperature and pressure are disturbed by the induced hydraulic fracture, the hydrate association rate can greatly increase. At the same time, the hydrate association could impose a weakening effect on the mechanical properties of the sediments. In general, the phase change of the gas hydrate is local and is affected by the fracture geometry of "wet" hydraulic fracture. Because the mechanical strength of NGH is generally larger than that of a sand skeleton, sand particle slippage can occur due to the local stress concentration; thus, sometimes the fracture initiation and propagation might be random. Moreover, because the rebuilding of new phase equilibrium balance needs time, the initiation and propagation are discontinuous and time-dependent. However, because only a rapid and intense phase change can create macro scope fractures, the majority of the created fractures due to phase change belong to the micro scope, while some of them do not connect together; however, this behavior could be more evident for the NGH samples with low gas hydrate saturation.

4.2 Fracture mode determination for NGH fracturing

The AE technology is not only able to realize the spatial evolution of hydraulic fractures but can also quantitatively identify the fracture morphology in the fracture mode through the AE parameters. The commonly used AE parameters mainly include the ringdown count, amplitude, rise time, energy rate, AE hits and so on (Miyazaki et al.,2011). To classify the fracture mode, the average frequency of AF (ringing count/duration) and the RA value (rise time/amplitude) are the most common methods. In general, tensile fractures result in an acoustic wave with high frequency and shorter duration, while shear fractures usually produces longer waveforms, with lower frequencies and longer rise times (Aggelis,2011; Bunger et al.,2014). After extracting the basic AE data of four AE parameters, including the ringdown count, duration, rise time and maximum amplitude, the RA value and average frequency AF of different hydraulic fracturing NGH samples can be obtained, as shown in Fig. 6. Fig. 6 (1) - (4) shows the fracture mode determination results for the NGH samples with high gas hydrate saturation. It has been seen that the fracture mode was composed of shear fractures and tensile fractures. In addition, the number of tensile fracture data points tends to be larger than that of shear fracture mode data, which demonstrates the tensile fractures are the dominate fracture type during NGH fracturing. Furthermore, under the slip-strike regime, the number of shear fracture mode data points seems to increase, demonstrating the creation of more complex fracture system. Fig. (5) ~ (8) illustrates the fracture mode for the NGH samples with low gas hydrate saturation by AE signals. According to the experimental results, the fracture modes also consist of shear fractures and tensile fractures but the number of shear fracture mode data points was larger than that of the tensile fracture mode. Unlike the AE behaviors for NGH samples with high gas hydrate saturation, shear fracture dominates the fracture mode for the NGH samples with low gas hydrate saturation, regardless of the in situ stress regime.

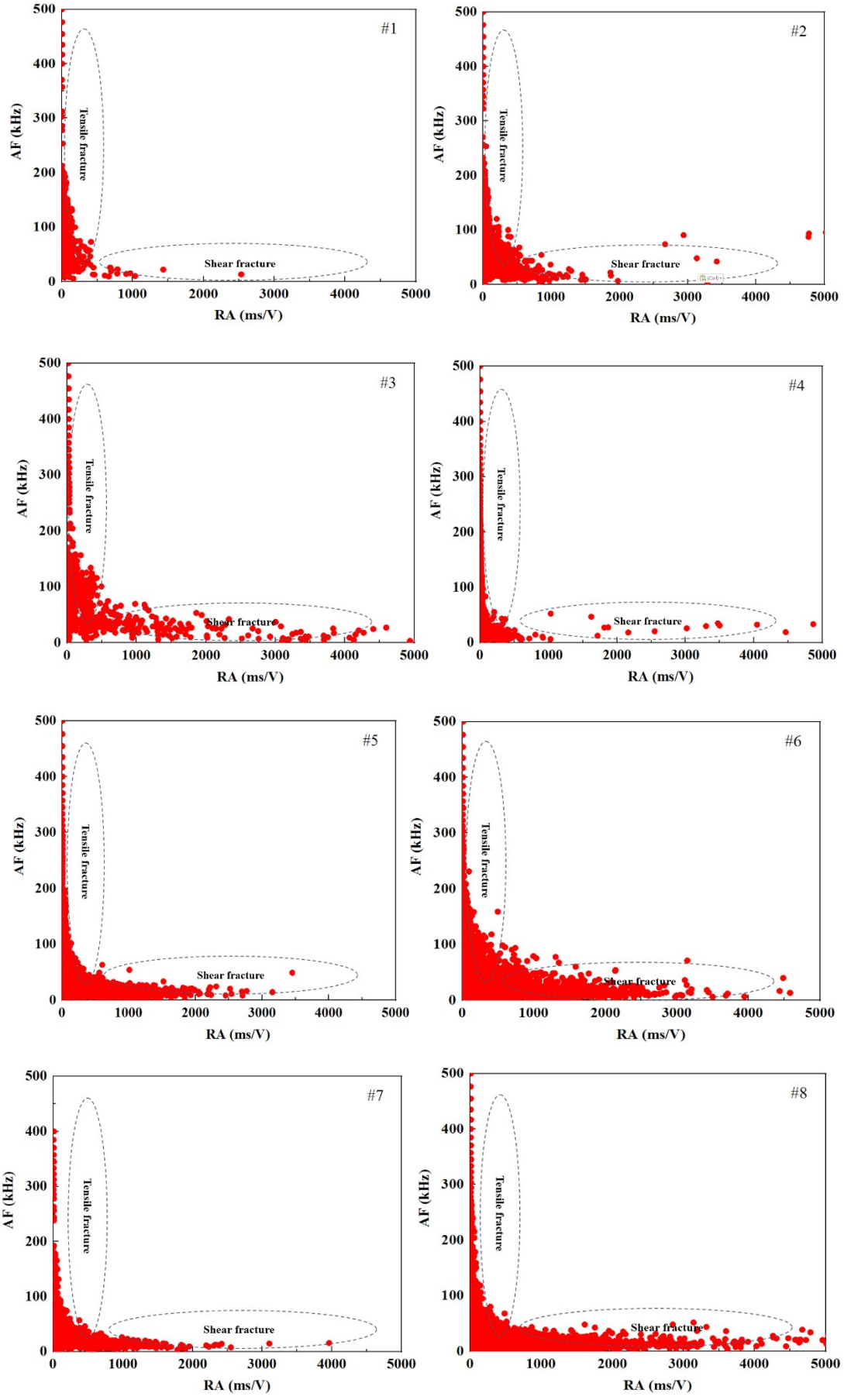

Fig. 6 Tensile and shear fracture mode determination for gas hydrate bearing sediment using acoustic emission technology

4.3 Hydraulic fracture mechanical stability analysis

Because of the pressure temperature dependent mechanical properties of the NGH samples, the mechanical stability of the hydraulic fracture is also of great concern for long-term production. Fig. 7 shows the fracture morphology for a sample after fracturing. Fig. 7(a) shows that the sample with high gas hydrate can be ignited by fire, indicating a rapid gas hydrate dissociation rate and an obvious permeability increase due to the created hydraulic fracture. Thus, the high effectiveness of hydraulic fracturing for samples with high gas hydrate can be validated. However, for the sample with low gas hydrate, ignition via fire is difficult. One reason stems from the less complex fracture system and another reason is the relatively low gas hydrate saturation. Because of the gas hydrate association, the mechanical strength of the NGH sample could degrade. Fig. 7(b) displays the fracture morphology for a sample with high gas hydrate saturation after full dissociation. It shows that the residual sample skeleton lost its bearing capability when the gas hydrate was fully decomposed. Moreover, detachment of the wellbore and sediment can be observed. The mechanical instability of the fractured NGH sample with high gas hydrate occurs mainly because the hydrate cementation effect plays a critical role in the intact sediment. When the solid gas hydrate converts into water and gas, a mechanical strength loss is inevitable. Fig. 7(c) shows the fracture morphology for a sample with low gas hydrate saturation after full dissociation. It can be seen that the whole NGH sediment is relatively intact after slickwater fracturing. Moreover, the wellbore is still detached from the NGH sediment, which indicates that the dissociation of the gas hydrate exerts less influence on the mechanical strength. The reason for these differences is the mechanical strength that is contributed by the solid hydrate to the NGH sediment with low gas hydrate saturation is less important than that for the NGH sediment with high gas hydrate saturation. Thus, when hydraulic fracturing treatments occur on the NGH zones with high gas hydrate saturation, the sharp reduction of mechanical properties will not only affect the fracture instability but also lead to greater risks in NGH development, such as sand production, borehole collapse and even the instability of hydrate barrier layer and submarine landslide. Compared to the stimulation on NGH reservoirs with high gas hydrate saturation, the hydraulic fracturing on NGH reservoirs with low gas hydrate saturation seems to be safer because of the small-scale deformation and failure, but the production rate can be avoided at the same time. Therefore, the design of a hydraulic fracturing stimulation process in an NGH reservoir should consider the competing effects between the stimulation effectiveness and safety.

(a) Burning sample with high gas hydrate saturation (from left to right: top view and side view)

(b) Fractured sample with high gas hydrate saturation after full dissociation

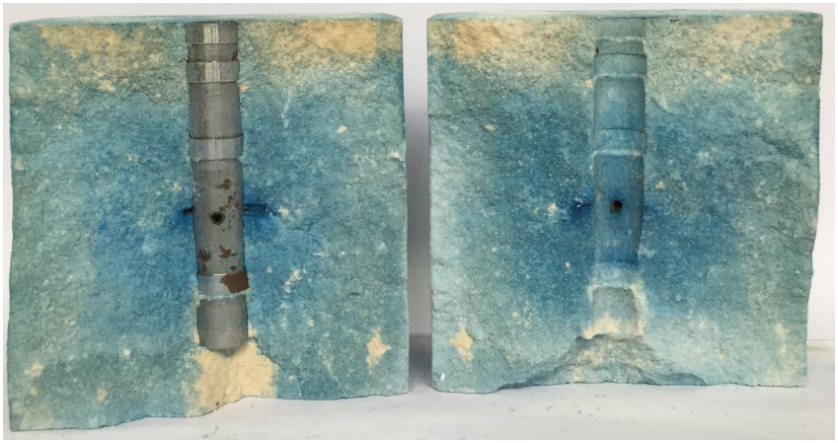

(c) Fractured sample with low gas hydrate saturation after full dissociation

Fig. 7 Fracture morphology after full dissociation

4.4 Microscopic observation of fractures under different disassociation times

The surface morphologies of NGH samples at the micro scale were recorded at 10 minutes, 2 hours, 12 hours and 24 hours after the hydrate fracturing, as shown in Fig. 8. It can be seen that significant bubbles appear instantaneously on the surface of NGH sediments after fracturing for 10 minutes. After 2 hours, these bubbles disappear while liquid flows then begin to appear on the surface. When the surface morphology is observed again after 12 hours and 24 hours, only the dry sediment skeleton can be seen. In particular, some sag and craters can be clearly observed on the local surface, which result from rapid gas hydrate decomposition and NGH sediment collapse. This appearance is remarkably similar to the field observations in gas hydrate rich areas that are located at the bottom of the Barents Sea and the permafrost area near the Arctic Circle (Andrrassen et al.,2017; Bogoyavlensky et al.,2019). Moreover, during the nonisothermal hydrate decomposition process, the temperature and pressure conditions near the main hydraulic fracture could be more intensively disturbed. The close observation of the fracture width showed that the fracture aperture varied along the fracture length, which might occur due to the different gas hydrate distributions. In addition, micro sand particles detached from sediments can be found, and these particles migrate into hydraulic fractures or micro cracks with the flow of gas or liquid, which can have a self-supporting effect on fracture conductivity endurance but could also be a risk for fracture clogs and sand production. Therefore, understanding the sand particle migration mechanism during hydraulic fracturing is critical for a proppant selection or proppant injection scenario.

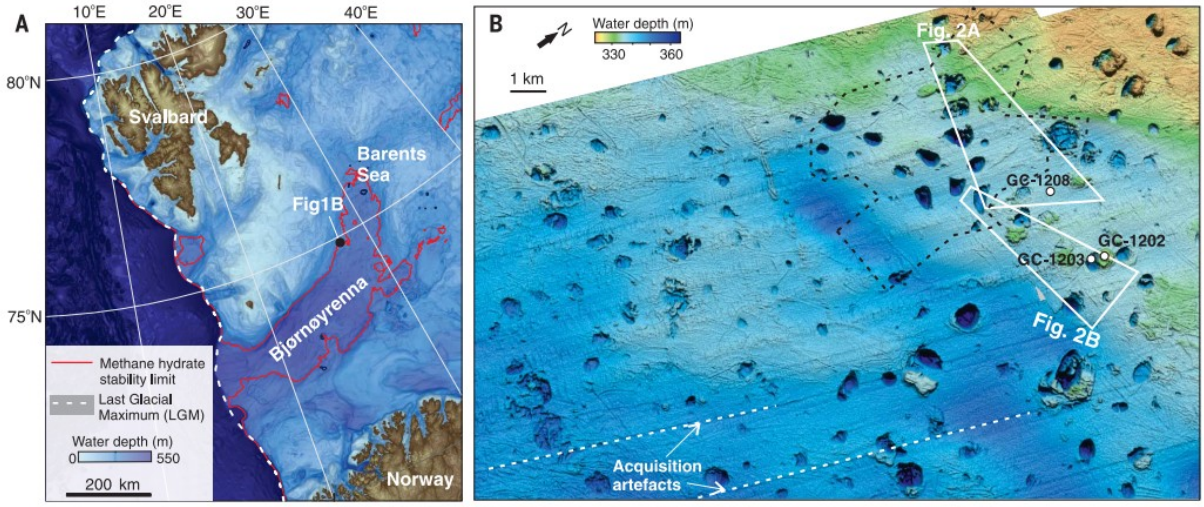

(a) Craters at the bottom of marine with different sizes (Andrrassen et al, 2017)

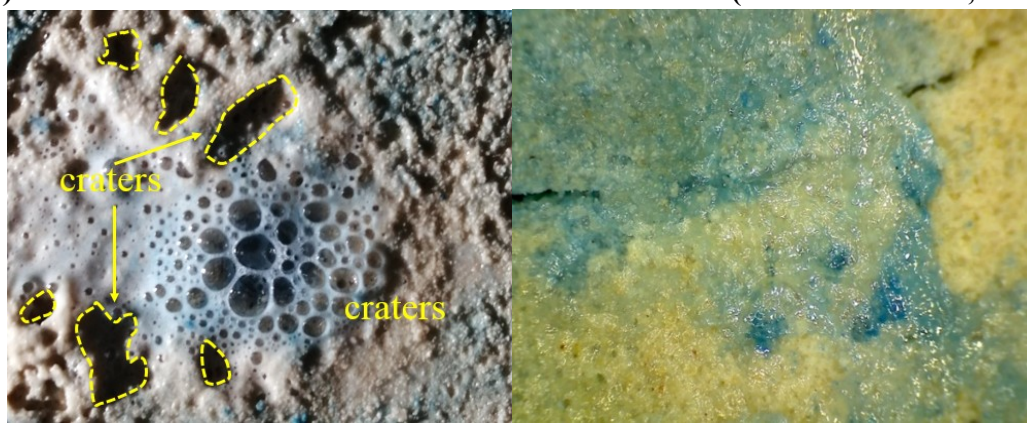

10 minutes **2 hours**

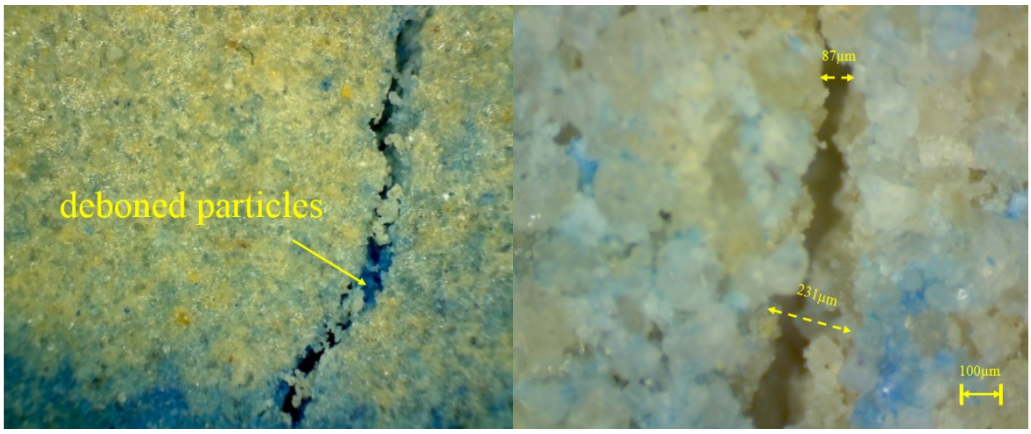

12 hours **24 hours**

(b) Fracture morphology change with time for NGH sample

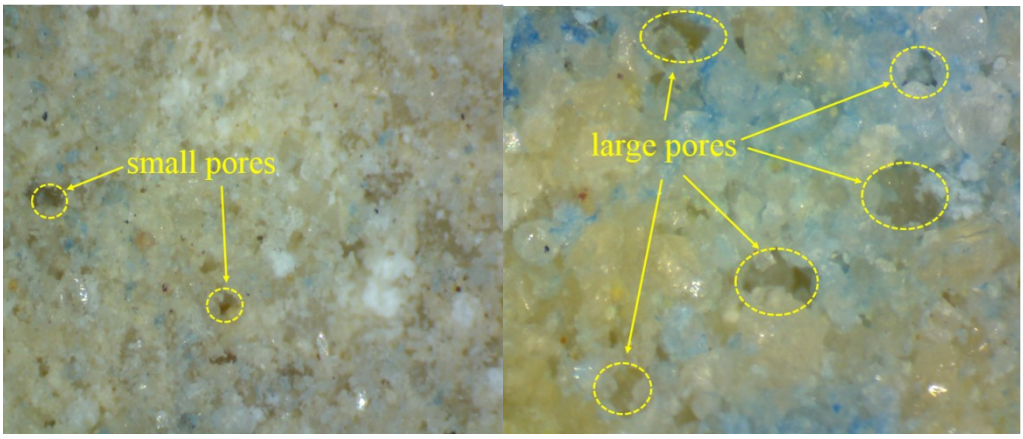

(c) Fracture morphology for NGH sample with low and high gas hydrate saturation after fully dissociation

(from left to right)

Fig. 7 Fracture morphology change with different dissociation time

Although the effectiveness of hydraulic fracturing in NGH development can be expected, some scholars believe that hydraulic fracturing may cause large-scale out-of-control decomposition of the gas hydrate, which is mainly because the physical and mechanical properties of NGHs are quite different from sedimentary rocks; thus, gas hydrate dissociation would cause a surge in the pore pressure and a decrease in the mechanical strength, which may induce seabed settlement and lead to slope collapse and instability and other geological disasters. More importantly, there are no strategies to remedy this situation if hydraulic fracturing begins. A previous study on the wellbore stability, sand production and the other engineering problems demonstrated the complex relationship between gas hydrate production and temperature pressure mechanical property alternation. Because of the larger contact area, there is no doubt that hydraulic fracturing in NGH reservoirs will increase gas hydrate dissociation more rapidly, which could bring more severe problems. Because there is no denying that safety and environmental protection are the primary prerequisites for the development of NGH resources, it is necessary to prevent hydraulic fracturing scale and reduce the risk of exploitation through an accurate hydraulic fracturing design by balancing the economic benefits and risks. Under the conditions of the existing technology, it is relatively feasible to assist gas hydrate dissociation through small-scale fracturing technology and the depressurization method, especially for the NGH reservoirs with stable boundary zones. Moreover, the fracturing fluid and proppant also need to be adopted and optimized to sustain the fracture closure, thus prolonging the effectiveness of hydraulic fracturing. It is believed that hydraulic fracturing is a potentially efficient technology to improve the hydrate development efficiency by an order of magnitude in the future.

5. Conclusions

By conducting tri-axial hydraulic fracturing laboratory experiments together with acoustic emission monitoring, this study validated the feasibility of using slickwater fracturing stimulation on NGH reservoirs under different gas hydrate saturations and in situ stress conditions. The following conclusions can be drawn:

(1) Under the stable thermodynamic condition for gas hydrate, the hydraulic fracture exert more obvious effects on gas hydrate dissociation for NGH samples with high gas hydrate saturation. On the other hand, the NGH samples with high gas hydrate saturation have better fracability

responses for fracturing stimulation. For the NGH samples with low gas hydrate saturation, the fluid invasion zone can be justified. Under the same conditions, the NGH samples under the normal fault regime are more likely to experience simple fractures, while the fracture geometries of the NGH samples under the strike-slip fault regime are more complex. Moreover, the lower horizontal stress difference not only increases the complexity of the fracture geometry but also increases the breakdown pressure

(2) According to the AE monitoring results, both the tensile and shear fracture modes can be determined during NGH fracturing, but the ratios of tensile and shear fracture modes are different with different gas hydrate saturations and in situ stress conditions. In general, the number of the shear fracture mode increases significantly with gas hydrate saturation. Moreover, a lower stress difference and the strike-slip fault regime are beneficial for shear fracture creation. The AE energy and three-dimensional location data with time indicate that a surge in the AE data also occurs after the injection stops, indicating the hysteresis effect for fracture initiation and an extension of the NGH fracturing. Thus, the phase change of the gas hydrate is an important fracture mechanism during NGH stimulation.

(3) The continuous observation of fracturing at the micro sale with time reveals that the hydraulic fracture stability changes with an unstable gas hydrate condition. Moreover, the local hydraulic fracture aperture is also affected by the gas hydrate distribution and dissociation degree. Although a large number of gas bubbles appear on the surface of the NGH sample with high gas hydrate saturation, a fast and gas hydrate decomposition induced by large strain and deformation can collapse the NGH sediment. Thus, in the absence of a stable boundary layer, the nondiagenetic hydrate reservoir with high saturation should use a small scale and accurate fracturing design. Moreover, the fracturing scenarios for NGH reservoirs should consider the contrasting effects between fracturing effectiveness and safety in advance.

Acknowledgments

The authors are grateful to the National Natural Science Foundation of China (51704324, 51374229), the Natural Science Foundation of Shandong Province (2019GGX103009, ZR2019MEE101), and the Fundamental Research Funds for the Central Universities (18CX02072A). Data used for this study can be accessed at https://osf.io/ws82b/files.

References

Aggelis, D. G. (2011). Classification of cracking mode in concrete by acoustic emission parameters. *Mechanics Research Communications*, 38, 153–157.

Andrrassen, K., Hubbard, A., Winsborrow, M., Patton, H., Vadakkepuliyambatta, S., Plaza-Faverola, A., et al. (2017). Massive blowout craters formed by hydrate-controlled methane expulsion from the Arctic seafloor. *Science*, 356(6341), 948–953.

Atousa, H., & Kiana, P. (2020). Study of biosurfactant effects on methane recovery from gas hydrate by CO_2 replacement and depressurization. *Fuel*, 272, 117681.

Bogoyavlensky, V. I., Sizov, O. S., Mazharov, A. V., et al. (2019). Earth degassing in the Arctic: remote and field studies of the Seyakha catastrophic gas blowout on the Yamal Peninsula. *The Arctic: Ecology and Economy*, 1(33), 88-105.

Boswell, R., Collett, T. S,. (2011). Current perspectives on gas hydrate resources. *Energy Environ Sci*, 4(4), 1206–15.

Bunger, A.P., Kear, J., Dyskin, A.V., Pasternak, E. (2014). Interpreting post-injection acoustic emission in laboratory hydraulic fracturing experiments. In: 48th US Rock Mechanics/Geomechanics Symposium. American Rock Mechanics Association.

Central Committee of CPC, State Council of PRC. (2017). The success of China's first exploring test on burning ice in marine area. People's Daily, 2017, 12.

Chen, B.B., Sun, H.R., Li, K.H., Wang, D.Y., Yang, M.J. (2019). Experimental investigation of natural gas hydrate production characteristics via novel combination modes of depressurization with water flow erosion. *Fuel*, 252, 295–303.

Chen, C., Yang, L., Jia, R., Sun, Y.H., Guo, W., Chen, Y., Li, X.T.(2017). Simulation study on the effect of fracturing technology on the production efficiency of natural gas hydrate. *Energies*, 10, 1241.

Chong, Z.R., Yang, S.H.B., Babu, P., Linga, P., Li. X-S. (2016). Review of natural gas hydrates as an energy resource: prospects and challenges. *Appl Energy*, 162, 1633–52.

Cranganu, C. (2009). In-situ thermal stimulation of gas hydrates. J Petrol Sci Eng, 65(1-2), 76–80.

Fakher, S., Abdelaal, H., Elgahawy, Y., Tonbary, A. E., Imqam, A. (2018). Increasing production flow rate and overall recovery from gas hydrate reservoirs using a combined steam flooding-thermodynamic inhibitor technique, In: SPE Trinidad and Tobago Section Energy Resources Conference (SPE 2018).

Falser, S., Uchida, S., Palmer, A. C., Soga, K., Tan, T.S. (2012). Increased gas production from hydrates by combining depressurization with heating of the wellbore. *Energy Fuels*, 26, 6259–67.

Feng, Y. C., Chen, L., Anna, S., Takuma, K., Junnosuke, O., Atsuki, K., et al. (2019). Enhancement of gas production from methane hydrate reservoirs by the combination of hydraulic fracturing and depressurization method. *Energ Convers Manage*, 184, 194–204.

Jin, Z.H., Johnson, S. E., Cook, A. E. (2015). Crack extension induced by dissociation of fracture-hosted methane gas hydrate. *Geophys. Res. Lett*, 42, 8522–8529.

Konno, Y., Jin, Y., Yoneda, J., Uchiumi, T., Shinjou, K., Nagao, J. (2016). Hydraulic fracturing in methane-hydrate-bearing sand. *RSC Adv*, 6, 73148–73155.

Li, B., Li, X. S., Li, G., Feng, J. C., Wang, Y. (2014). Depressurization induced gas production from hydrate deposits with low gas saturation in a pilot-scale hydrate simulator. *Appl Energy*, 129, 274–86.

Miyazaki, K., Masui, A., Sakamoto, Y., Aoki, K., Tenma, N., Yamaguchi, T. (2011). Triaxial compressive properties of artificial methane-hydrate-bearing sediment. *J. Geophys. Res,* B06102.

Oyama, H., Konno, Y., Masuda, Y., Narita, H. (2009). Dependence of depressurization-induced dissociation of methane hydrate bearing laboratory cores on heat transfer. *Energy Fuels*, 23(10), 4995−5002.

Piñero, E., Marquardt, M., Hensen, C., Haecke,l M., Wallmann, K. (2016). Estimation of the global inventory of methane hydrates in marine sediments using transfer functions. *Biogeosciences*, 10, 959–75.

Qazi, N., Humbul, S., Yasir, A., Elsheikh. (2020). A review on the role and impact of various additives as promoters/inhibitors for gas hydrate formation. *J Nat Gas Sci Eng* ,76, 103211.

Rachel, F. W., Samuel, M. T., Nigel, J. C. (2017). A sensitivity analysis of the effect of pumping parameters on hydraulic fracture networks and local stresses during shale gas operations. *Fuel*, 203, 843–852.

Song, Y., Cheng, C., Zhao, J., Zhu, Z., Liu, W., Yang, M., et al. (2015). Evaluation of gas production from methane hydrates using depressurization, thermal stimulation and combined methods. *Appl Energy*, 45, 265–77.

Too, J. L., Cheng, A., Khoo, B. C., Palmer, A., Linga, P. (2018). Hydraulic fracturing in a penny-shaped crack. part ii: testing the frackability of methane hydrate-bearing sand. *J Nat Gas Sci Eng*, 52, 619-628.

Too, J. L., Cheng, A., Khoo, B. C., Palmer, A., Linga, P. (2018). Hydraulic fracturing in a penny-shaped crack. Part II: Testing the frackability of methane hydrate-bearing sand. *J Nat Gas Sci Eng*, 52, 619–628.

Wang, Z.Y., Liao, Y. Q., Zhang, W. D., Sun, B. J., Sun, X. H., Deng, X. J. (2018). Coupled temperature field model of gas-hydrate formation for thermal fluid fracturing. *Appl Therm Eng*, 133, 160–169.

Xu, C. G., & Li, X. S. (2018). Research progress on methane production from natural gas hydrates. *RCS Adv*, 5, 54672–99.

Yohan, L., Wonjung, C., Kyuchul, S., Yongwon, S. (2017). CH_4-CO_2 replacement occurring in sII natural gas hydrates for CH_4 recovery and CO_2 sequestration. *Energy Conversion and Management*, 150, 356–364.

Zhang, X. H., LU, X. B., LI, P. (2019). A comprehensive review in natural gas hydrate recovery methods. *Sci Sin-Phys Mech Astron*, 49, 034604.

Zhang, X. W., Lu, Y. Y., Tang, J. R., Zhou, Z., Liao, Y. (2017). Experimental study on fracture initiation and propagation in shale using supercritical carbon dioxide fracturing. *Fuel*, 190, 370–378.